Metabolic Dependency Shapes Bivalent Antiviral Response in Host Cells: The Role of Glutamine

Grégorie Lebeau[1], Aurélie Paulo-Ramos[2], Mathilde Hoarau[2], Daed El Safadi[1], Olivier Meilhac[2], Pascale Krejbich-Trotot[1], Marjolaine Roche[1] and Wildriss Viranaicken[1,2]*

[1] Université de la Réunion, INSERM U1187, CNRS UMR 9192, IRD UMR 249, Unité Mixte Processus Infectieux en Milieu Insulaire Tropical, Plateforme Technologique CYROI, 94791 Sainte Clotilde, La Réunion, France

[2] Université de La Réunion, INSERM, UMR 1188 Diabète athérothombose Réunion Océan Indien (DéTROI), Campus Santé Université de la Réunion, 77 avenue du Docteur Jean-Marie Dambreville, 97410 Saint-Pierre, France

* Correspondence: gregorie.lebeau@univ-reunion.fr (G.L.)

Abstract: The establishment of effective antiviral responses within host cells is intricately related to their metabolic status, shedding light on immunometabolism. In this study, we investigated the hypothesis that cellular reliance on glutamine metabolism contributes to the development of a potent antiviral response. We evaluated the antiviral response in the presence or absence of L-glutamine in the culture medium, revealing a bivalent response hinging on cellular metabolism. While certain interferon-stimulated genes (ISGs) exhibited higher expression in an oxidative phosphorylation (OXPHOS)-dependent manner, others were surprisingly upregulated in a glycolytic-dependent manner. This metabolic dichotomy was influenced in part by variations in IFN-β expression. We initially demonstrated that the presence of L-glutamine induced an enhancement of oxidative phosphorylation in A549 cells. Furthermore, in cells stimulated poly:IC, a marked increase in ISGs expression was observed in a dose-dependent manner with L-glutamine supplementation. Interestingly, our findings unveiled a metabolic dependency in the expression of specific ISGs. In particular, genes such as ISG54, ISG12 and ISG15 exhibited heightened expression in cells cultured with L-glutamine, corresponding to higher OXPHOS rates and IFN-β signaling. Conversely, the expression of viperin and 2'-5'-oligoadenylate synthetase 1 was inversely related to L-glutamine concentration, suggesting a glycolysis-dependent regulation, confirmed by inhibition experiments. This study highlights the intricate interplay between cellular metabolism, especially glutaminergic and glycolytic, and the establishment of the canonical antiviral response characterized by the expression of antiviral effectors, potentially paving the way for novel strategies to modulate antiviral responses through metabolic interventions.

Keywords: antiviral response, OXPHOS, mitochondrial respiration, glycolysis, metabolic reprogramming, immunometabolism

Abbreviations

2-DG	2-deoxyglucose
A549^{Dual}	A549-Dual™, expressing NF-κB-SEAP and IRF-Luc reporters
GAS	Gamma interferon activation site
IFN	Interferon
IFNAR	IFNs α/β receptor
IRF	Interferon Regulatory Factor
ISG	Interferon Stimulated Gene
ISRE	IFN-stimulated response element
mROS	Mitochondrial reactive oxygen species
OXPHOS	Oxidative phosphorylation
PIC	Poly(I:C) (HMW) / LyoVec™

1. Introduction

Over the past two decades, we have been regularly confronted with our vulnerability to infectious diseases, whether emerging or re-emerging [1–7]. To deal with epidemics that can take on worldwide proportions, major research efforts have been required to gain a better understanding, not only of the emergence of these viruses, but also the pathophysiology associated with them. The antiviral response is one of the most widely explored aspects, depicting the host-pathogen relationship that develops during infection, which represents an evolutionary mechanism elaborated by the host to struggle against viral infections [8]. The canonical pathway of the antiviral response - the Interferon (IFN) pathway - is initiated by the recognition of pattern associated molecular patterns (PAMPs), usually viral nucleic acids, by pattern recognition receptors (PRRs). The viral genome released into the cytosol is specifically recognized by RIG-I like receptors (RLR *e.g.*, RIG-I and MDA5) notably for viral 5'PPP-RNA and cyclic GMP-AMP Synthase (cGAS) for viral dsDNA [9,10]. Nucleic acids of endosomal origin are recognized by Toll-like receptors (TLRs) found in the endosome; TLR3 for dsRNA, TLR7/8 for ssRNA and TLR9 for DNA containing unmethylated CpGs [9]. Most of these receptors activate interferon regulatory factors (IRFs) via adaptor proteins. For example, RIG-I and MDA5 interact with MAVS via their CARD domain, leading to a signaling cascade involving TRAF3, TBK1 and IKKε, resulting in phosphorylation and heterodimerization of IRF7 and IRF3 [9]. Similarly, TLR3, via TRIF, leads to activation of IRF3 and 7 while TLR7, 8 and 9, via MYD88, lead to the formation of IRF7 homodimers [9]. More recently, the demonstration of the ability of cGAS to produce cyclic GMP-AMP (cGAMP) following the detection of cytosolic dsDNA led to the description of a new IFN production pathway, via the Stimulator of Interferon Genes – STING [10]. STING, through TBK1, leads to phosphorylation and homodimerization of IRF3 [10]. Finally, IRFs activated by these different pathways can translocate to the nucleus of the infected cell, where they interact with their promoter to allow transcription of type I and III IFNs. It is difficult to distinguish the intrinsic activity of type I IFNs (predominantly β) from type III IFNs, as their secretion occurs concomitantly [11]. Secreted IFNs act in an autocrine and paracrine manner, via their IFNAR1/2 and IFNLR1/IL-10Rβ receptors respectively, leading to the phosphorylation and homodimerization of STAT1 (GAF) on the one hand and, on the other, to the formation of the ISGF3 complex, composed of IRF9 and phosphorylated STAT1 and 2 [11,12]. ISGF3 interacts with the interferon-sensitive responsive element (ISRE), while GAF interacts with the gamma interferon activation site (GAS), in both cases leading to the expression of ISGs [11,12]. Alternatively, specific antiviral programs have been demonstrated, involving, for example, peroxisomal localization of MAVS which, after interaction with RIG-I, specifically induces activation of IRF1 leading to direct expression of antiviral genes and, at epithelial level, IFN-λ [13,14]. The interferon-stimulated genes (ISGs) encode antiviral proteins that have various functions on the virus life cycle, including inhibition of viral entry (myxovirus resistance genes), translation and replication (IFIT family, viperin), or even budding (tetherin) [11]. Additionally, they are able to improve sensing or potentiate interferon signaling pathways [15].

The IFN response is acute, representing the first line of defense deployed by cells at the site of infection, limiting the spread of the virus throughout the body. It also enables the innate and adaptive immune responses to be established accordingly [16]. However, this line of defense is vulnerable and many viruses have developed mechanisms to circumvent and control the antiviral response. To avoid the IFN response, several of these mechanisms are often active simultaneously. Upstream of IFN secretion, certain viruses appear to act by limiting the detection of their genome or by interfering with the signaling pathways leading to IFN secretion. For example, the N and NSP5 proteins of

SARS-CoV-2 limit the polyubiquitination of RIG-I, which is involved in the stabilization of its CARD domains and the aggregation of MAVS [17]. Viral protease from HCV has shown the ability to cleave Cardif an adaptor protein in the RIG-I antiviral pathway [18]. Viral escape can also occur downstream of IFN secretion by inhibiting ISG production. Many viruses (*e.g.*, Nipah virus, Measles virus, DENV, ZIKV) are able to target STAT1 and STAT2, sequestering them or causing their degradation [19]. Furthermore, while metabolism has proven to be of interest in the activation of immune cells [20], it is no less central to the IFN response. Metabolism is a crucial control point for the virus during infection in several regards. Firstly, during infection, the diversion of cellular metabolism from oxidative phosphorylation to glycolysis, via a Warburg-like effect, allows the virus to access a quantity of biomass consistent with viral progeny [21]. On the other hand, control of metabolism could limit its effects on the establishment of the antiviral response. Indeed, we have previously shown that induction of the antiviral response by poly:IC in galactose-cultured cells, to boost their oxidative phosphorylation, resulted in greater expression of ISGs than when cells based their metabolism on glucose use and glycolysis [22]. Consistent with our results, mitochondrial ROS production was previously shown to induce MAVS oligomerization and type I IFN production [23]. In support of this hypothesis, it was shown that cells resistant to HIV-induced aerobic glycolysis have a higher antiviral potential and are accompanied by virus control [24]. Strengthening the link between cell respiration and virus infection, flavivirus affects the respiratory pathways of infected cells, notably through inhibition of mitochondrial fission by NS4B, which prevents the onset of mitochondrial antiviral status due to decreased ROS production [25,26]. Additionally, illustrating the deleterious effect of aerobic glycolysis on infected cells, the lactate produced by this process has been shown to affect RIG-I-dependent IFN production by regulating MAVS [27].

It has been stated on several occasions that the supply of TCA and therefore of oxidative phosphorylation can occur through the anaplerotic use of glutamine to give α-ketoglutarate. However, to date, the beneficial effect of glutamine during infection remained unclear. Indeed, it has been suggested that infected cells may be 'addicted' to glutamine, although it has not been established whether this addiction is due to the virus or rather to the requirement for glutamine to mount an effective antiviral response [28]. The work of Shiratori et al. illustrates that the use of galactose to force the metabolic reprogramming of cancer cells toward OXPHOS relies on increasing the glutamine pool to anaplerotically generate TCA intermediates [29]. In light of these data and our previous work, we hypothesize here that the host cell depends on glutamine to establish a metabolic process adapted to the development of an effective antiviral response. To test this hypothesis, we decided to evaluate the antiviral response in the presence or absence of L-glutamine in our culture medium. Interestingly, we demonstrated the existence of a bivalent antiviral response depending on cellular metabolism. Indeed, some ISGs are more expressed in an OXPHOS-dependent manner, as we expected, while others are more expressed in a glycolytic-dependent manner, the dichotomy in part relying on a variation of IFN-β expression.

2. Materials and methods

2.1. Cells and reagents

The human A549-Dual™ ($A549^{Dual}$) are adherent epithelial cells derived from A549 lung carcinoma cell line (ATCC, CCL-185™). $A549^{Dual}$ were purchased from InvivoGen (ref. a549d-nfis, San Diego, CA, USA). QUANTI-Luc™ substrate was obtained from InvivoGen (ref. rep-qlc1, San Diego, CA, USA). Oligomycin (ref. 75351), myxothiazol (ref. T5580), 2-deoxyglucose (2-DG, ref. D8375), 2,4-dinitrophenol (DNP, ref. D198501) and rotenone (ref. R8875) was purchased from

Sigma-Aldrich (Saint-Louis, MO, USA). Poly(I:C) (HMW) / LyoVec™ (PIC) was purchased from InvivoGen (ref. tlrl-piclv, San Diego, CA, USA). MitoSOX™ Red was purchased from InvitroGen (ref. M36008, Carlsbad, CA, USA). Non-essential amino acid solution was purchased from PAN Biotech (ref. P08-32100, Aidenbach, Germany).

2.2. Cell culture

A549^{Dual} cells were cultured for maintenance at 37°C under a 5% CO_2 atmosphere in 4,5 g·L^{-1} glucose Dubecco's Modified Eagle's Medium – DMEM (PAN Biotech, Aidenbach, Germany) supplemented with 10% of heat-inactivated fetal bovine serum (FBS, Dutscher, Brumath, France), 100 U·mL^{-1} penicillin, 100 µg·mL^{-1} streptomycin, 2 mM L-glutamine and 0.5 µg·mL^{-1} amphotericin B (PAN Biotech, Dutsher, Brumath, France) and containing 10 µg·mL^{-1} blasticidin and 100 µg·mL^{-1} zeocin (InvivoGen, San Diego, CA, USA), for selection of cells expressing NF-κB-SEAP and IRF-Luc reporters.

2.3. Oxygen consumption rate assessment

A549^{Dual} cells were cultured in 25 cm^2 flasks, DMEM 4.5 g·L^{-1} glucose was replaced by RPMI 2 g·L^{-1} glucose, supplemented or not with 2 mM L-glutamine 24 hours before oxygen consumption rate (OCR) assessment. The cells were then washed with PBS, collected with trypsin / EDTA, and centrifuged at 800×*g* for 5 min, at room temperature. Subsequently, cell pellets were suspended in a volume of RPMI 2 g·L^{-1} glucose, supplemented or not with 2 mM L-glutamine, allowing the number of cells per chamber to be standardized (approximately 2×10^6 cells). Basal oxygen consumption rates were continuously measured on whole cells at 37°C, using a Clark-type oxygen electrode (Oroboros Oxygraph-2k, Oroboros Instruments, Innsbruck, Austria). For calibration of the polarographic oxygen sensor and measurement of background oxygen consumption, the medium without biological sample was added to the O2k-chamber. For each experimental condition, OCR was measured in the presence or absence of the F1F0-ATP synthase inhibitor – oligomycin (1 µM), the glycolysis inhibitor – 2-DG (5 mM), the protonophoric uncoupler – dinitrophenol (100 µM) and a mix of the mitochondrial complex III inhibitor – myxothiazol (1 µM) and the mitochondrial complex I inhibitor – rotenone (1 µM). Data were expressed as picomoles O_2 consumed by cells per second and per million of cells.

2.4. Cytotoxicity assay

A549^{Dual} were plated in 96-well plate with a density of seeding corresponding to 10,000 cells per well. Cells were then treated respectively with RPMI 2 g·L^{-1} glucose, supplemented (or not) with 2-mM L-glutamine, containing increasing doses of 2-DG (ranging from 1 mM to 20 mM). DMEM – DMSO 10% was used as a positive death inductor. 24 hours after, cells undergo for neutral red assay.

Cell viability was assessed with neutral red uptake assay, as described by Repetto et al. [30]. Briefly, after removal of the cell culture supernatant, 100 µL of medium containing 40 µg·mL^{-1} of neutral red was added to each well. Cells were then incubated during 2 hours at 37°C. Following incubation, medium was removed and cells were washed with PBS. Finally, 150 µL of neutral red destain (50% ethanol, 49% H2O, 1% glacial acetic acid) was added to each well. Absorbance was read at 540 nm using FLUOstar® Omega microplate reader (BMG LABTECH, Offenburg, Germany).

$$Cell\ viability\ (\%) = 100\ \times \frac{Experimental\ condition\ (OD_{540})}{Negative\ control\ (OD_{540})}$$

2.5. Cell stimulation

Antiviral response was induced using polyriboinosinic:polyribocytidylic acid (poly:IC), a double stranded RNA complexed with transfection reagents which improve its uptake. A549^{Dual} were cultured in RPMI-1640 (ref. P04-17550, PAN Biotech, Aidenbach, Germany) supplemented with glucose (2 g·L^{-1}) and with or without L-glutamine upon stimulation, to promote metabolic reprogramming. Briefly, cells were plated in RPMI-1640 supplemented with 10% FBS containing 2 g·L^{-1} of glucose with L-glutamine at different concentrations (0 mM, 0.2 mM, 1 mM or 2mM). After 24 hours of adaptation, cells were stimulated during 6 hours using PIC at 0.25 µg·mL^{-1} to study early steps of IFN pathway and 24 hours for late steps of IFN pathway (*e.g.*, ISGs production). In the same manner, assessment of antiviral response following cellular respiration or glycolysis inhibition was achieved using 0.25 µg·mL^{-1} PIC and respectively 1 µg·mL^{-1} rotenone or 5 mM 2-DG during 24 hours on A549^{Dual} either cultured in RPMI-1640 with 2 g·L^{-1} glucose either supplemented with L-glutamine 2 mM or not for 24 hours. Following stimulation, cell culture supernatant was harvested and stored at -20°C, while cells were either used fresh in flow cytometry, fixed for immunofluorescence or lysed using RLT Lysis Buffer (Qiagen, Hilden, Germany) for subsequent RNA extraction or using RIPA buffer for subsequent protein preparation.

2.6. RT-qPCR

Total RNA has been extracted from cell lysates by using the RNeasy Plus Mini Kit (cat. 74136, Qiagen, Hilden, Germany). The total cDNA was obtained by reverse transcription using random primers from Invitrogen (ref. 58875, ThermoFisher, Waltham, MA, USA) and M-MLV reverse transcriptase enzyme (ref. M1708, Promega, Madison, WI, USA) at 42 °C for 60 minutes. cDNA was then subjected to a quantitative polymerase chain reaction, using a CFX96 Connect™ Real Time Detection System (Bio-Rad, Hercule, CA, USA). For amplification, BlasTaq™ 2X qPCR MasterMix (ref. G892-1, Applied Biological Materials, Vancouver, Canada) and specific primers were used to assess gene transcripts expression for following targets: ISG56, ISG54, ISG15, ISG12, IRF1, Viperin, OAS1, CMPK2, lncRNA-NRIR, IFN-β, RNA polymerase II and 18S ribosomal RNA. A threshold cycle (Ct) was calculated for each single sample amplification reaction in the exponential phase of amplification, using Bio-Rad CFX Manager 3.1 (Bio-Rad, Hercule, CA, USA). Data obtained were expressed as mean normalized expression, RNA polymerase II and 18S ribosomal RNA serving has housekeeping gene.

Gene	Forward primer	Reverse primer
RNA polymerase II	5'-GAGAGCGTTGAGTTCCAGAACC-3'	5'-TGGATGTGTGCGTTGCTCAGCA-3'
18S ribosomal RNA	5'-AGCCTGCGGCTTAATTTGAC-3'	5'-CAACTAAGAACGGCCATGCA-3'
ISG56	5'-GCAGCCAAGTTTTACCGAAG-3'	5'-CACCTCAAATGTGGGCTTTT-3'
ISG54	5'-CTGGTCACCTGGGGAAACTA-3'	5'- GAGCCTTCTCAAAGCACACC-3'
ISG15	5'-AGATCACCCAGAAGATCGGC-3'	5'-GAGGTTCGTCGCATTTGTCC-3'
ISG12	5'-CGTCCTCCATAGCAGCCAAGAT-3'	5'-ACCCAATGGAGCCCAGGATGAA-3'
IRF1	5'-GAGGAGGTGAAAGACCAGAGCA-3'	5'-TAGCATCTCGGCTGGACTTCGA-3'
Viperin	5'-GATGTTGGTGTAGAAGAAGC-3'	5'-CCAATCCAGCTTCAGATCAG-3'
OAS1	5'-CATGCAAATCAACCATGCCA-3'	5'-ACAACCAGGTCAGCGTCAGATC-3'
CMPK2	5'-CCAGGTTGTTGCCATCGAAG-3'	5'-CAAGAGGGTGGTGACTTTAAGAG-3'
lncRNA-NRIR	5'-CCACCCCCACGAAGAAATTATATATC-3'	5'-GTTAGAGGTGTCTGCTGCAATAATC-3'
IFN-β	5'-CTTGGATTCCTACAAAGAAGCAGC-3'	5'-TCCTCCTTCTGGAACTGCTGCA-3'

2.7. Western blot

Stimulated cells (see *2.4 Cell stimulation*) were lysed in 200 µL of radioimmunoprecipitation assay buffer (RIPA buffer) at 4 ° C for 10 min. Lysate were sonicated at 0 °C for 1 min of pulse at 40% at 0.5 cycle using an Omni-Ruptor

4000 (Omni International, Dutscher, Issy-les-Moulineaux, France). Proteins from total cell extract were quantified using BCA reagent according to manufacturer instructions (Sigma-Aldrich, Humeau, La Chapelle-Sur-Erdre, France). A standardized amount of protein extracts was treated with Laemmli buffer containing 10 mM DTT and heated at 95 ° C for 5 min. 15 µg of proteins were separated on precast NuPAGE gels 4 – 12% (Thermofischer, France) at 200V constant for 35 minutes. Transfer was performed on NC Protan supported membrane with a 0.45 µm pores (Amersham, GE, Buc, France) at 60 mA constant per gel for 2 hours using a semi-dry system. After transfer, the membranes were saturated with 5% nonfat dry milk in PBS – Tween 0.1%. Membranes were then incubated successively with primary antibodies and secondary antibodies diluted in PBS – Tween 0.1% – 1% nonfat dry milk. Blots were revealed with enhanced chemiluminescence, ECL prime detection reagents (GE, Buc, France) using an Amersham Imager 680 (GE, Buc, France).

Target	Reference	Dilution
Rabbit anti-ISG15	MA5-29371 (Invitrogen)	1:1000
Mouse anti-ISG56	MA5-25050 (Invitrogen)	1:1000
Mouse anti-Viperin	MABF106 (Sigma-Aldrich)	1:1000
Mouse anti-IFN-β	AB_2122765 (Biolegend)	1:1000
Rabbit anti-pSTAT2	07-224 (Sigma-Aldrich)	1:1000
Rabbit anti-β-Tubulin	AC008 (ABclonal)	1:1000
Goat anti-rabbit immunoglobulin-HRP	AB_2313567 (Jackson ImmunoResearch)	1:5000
Goat anti-mouse immunoglobulin-HRP	AB_10015289 (Jackson ImmunoResearch)	1:5000

2.8. Mitochondrial ROS measurement

Mitochondrial ROS were measured with MitoSOX™ Red using a flow cytometry-based protocol [31]. Briefly, A549^{Dual} were washed with PBS 1X, harvested with trypsin / EDTA, and centrifuged at 800×*g* for 5 min. After three washes, cells were resuspended in preheated RPMI 2 g·L^{-1} glucose without phenol red, supplemented or not with 2 mM L-glutamine. MitoSOX™ Red at a final concentration of 5 µM was added to cell suspension and incubated for 30 min at 37°C. After three washes with preheated medium, the expression of MitoSOX™ is quantified in the PE channel by flow cytometry, using a CytoFLEX (Beckman Coulter, CA, USA).

2.9. Immunofluorescence

A549^{Dual} cells grown on glass coverslips were fixed with 3.7% paraformaldehyde – 50 mM HEPES – 150 mM NaCl at room temperature for 10 min. Fixed cells were permeabilized with 0.1% Triton X-100 in PBS for 3 min. The coverslips were incubated with primary antibodies in 1% BSA – PBS. Antigen – antibody binding was visualized with donkey anti-mouse Alexa 488 Fluor-conjugated and donkey anti-rabbit Alexa 488 Fluor-conjugated secondary antibodies. Nucleus morphology was revealed by 4,6-Diamidino-2-phenylindole dihydrochloride (DAPI) staining. The coverslips were mounted with ibidi Mounting Medium (ref. 50001, ibidi, Gräfelfing, Germany) and fluorescence was observed using an AXIO OBSERVER 7 equipped with the Apotome.2 (Zeiss, Oberkochen, Germany). The images were acquired with the ZEN software version 3.1 (Zeiss, Oberkochen, Germany).

Target	Reference	Dilution
Mouse anti-TOM20	sc-17764 (Santa Cruz)	1:200
Mouse anti-IFN-β	AB_2122765 (Biolegend)	1:200
Rabbit anti-STAT2	sc-22816 (Santa Cruz)	1:200
Donkey anti-mouse Alexa 488	ab150105 (abcam)	1:750
Donkey anti-rabbit Alexa 488	ab150073 (abcam)	1:750

2.10. Measurement of the IFN-β Pathway activation

Activation of the Interferon regulatory factors (IRF) pathway was monitored by measuring Lucia luciferase activity in A549^{Dual} cells. It was evaluated using QUANTI-Luc substrate according to manufacturer's recommendations. Briefly, 100 µL of QUANTI-Luc substrate was added to 20 µL of cell culture supernatant and IRF-induced luciferase levels were quantified by luminescence measurement using a Luminoskan™ microplate luminometer (ThermoFisher, Waltham, MA, USA).

2.11. Transcription factors prediction

Prediction of potential binding sites for transcription factors in the promoter region of antiviral effectors was achieved using PROMO tool from ALGGEN group, which based on TRANSFAC 8.3 [32,33]. Briefly, a sequence of at least 1000 bp upstream of the 1st exon of each of the following genes was recovered from the Ensembl database [34]: viperin (ENSG00000134321), OAS1 (ENSG00000089127), ISG12 (ENSG00000165949), ISG15 (ENSG00000187608) and ISG54 (ENSG00000119922). These sequences were submitted to MultiSearchSites to search for binding sites that viperin and OAS1 sequences share on the one hand and ISG12, ISG15, and ISG54 on the other, restricting the prediction to the human set of transcription factors. A Venn diagram was then drawn to illustrate the transcription factors common or specific to these groups [35].

2.12. Statistical analyses

For all figures except figures 1 and 2C, statistical analyses were performed by two-way ANOVA with Dunnett's correction using Graph-Pad Prism software version 9. For figures 1 and 2C, statistical analyses were done using unpaired T-test. Values of $p<0.05$ were considered statistically significant. The degrees of significance are indicated in the figures captions as follow: *$p<0.0332$; ** $p<0.0021$; *** $p<0.0002$; **** $p<0.0001$.

3. Results

3.1. Enhancement of OXPHOS occurs in presence of L-glutamine

We have previously demonstrated the ability of cells to produce a more effective antiviral response if cellular respiration was increased [22]. We then induced metabolic reprogramming of our cells using galactose. Galactose was shown to anaplerotically feed TCA via L-glutamine production [29]. An open question in the literature is whether L-glutamine is essential for antiviral response or viral progeny [28]. In light of our previous results, we hypothesized that L-glutamine would be essential for the establishment of an effective antiviral response, via the supply of TCA and OXPHOS.

As a first step, we therefore evaluated the ability of L-glutamine to induce an increase in cellular respiration. To do so, we cultured A549^{Dual} cells in RPMI containing 2 $g \cdot L^{-1}$ glucose, supplemented or not with 2 mM L-glutamine. After 24h of adaptation, we measured the O_2 consumption of our cells by oximetry, using different uncoupling agents. As shown in **Figure 1A**, our two culture conditions lead to a different O_2 consumption rate. Indeed, the basal level of O_2 consumption is significantly increased in the presence of L-glutamine **(Figure 1B - left panel)**. Moreover, using 2,4-dinitrophenol to force the passage of protons from the mitochondrial intermembrane space reveals that the maximal respiratory capacity of A549^{Dual} is also significantly increased – 40% higher – in the presence of L-glutamine **(Figure 1B – middle panel)**. Finally, we measured the proportion of O_2 consumption not attributable to mitochondria, completely uncoupling the mitochondrial respiratory chain using a mixture of rotenone and myxothiazol. Cells grown without L-

glutamine showed greater non-mitochondrial cellular respiration than cells grown in the presence of L-glutamine **(Figure 1B - right panel)**. Notably, the proton leakage assessed through the use of oligomycin was not different between our two culture conditions. Also, the use of 2-deoxyglucose (2-DG) induces a decrease in O_2 consumption but with no significant difference between cells cultured with or without L-glutamine. Thus, we have shown that L-glutamine induces an increase in cellular respiration in $A549^{Dual}$ which, according to our hypothesis, could be associated with a greater antiviral response in an infectious context.

3.2. The antiviral response is bivalent and varies according to metabolic context

As mentioned above, the role of L-glutamine in infection is not well defined yet. Some believe that L-glutamine is essential for virus progeny, making the virus addicted to L-glutamine [28]. Others suggest that L-glutamine is necessary for the antiviral response, making the host cell addicted to L-glutamine during infection. Assuming that L-glutamine supports a metabolism based on oxidative phosphorylation, it seems reasonable to suppose that it would also support the development of the antiviral response. In order to prove the host cell's addiction to L-glutamine for the development of the antiviral response, we decided to use poly:IC (PIC) with increasing doses of L-glutamine. PIC is a dsRNA, widely used as pathogen associated molecular pattern mimetic. Indeed, It is known to mimic replicating viral RNA and to trigger the antiviral response, through activation of TLR3, RIG-I and RIG-I like receptors (RLR), resulting in type I IFNs production and ISGs expression [36,37].

Thus, we cultured $A549^{Dual}$ with increasing doses of L-glutamine (from 0 to 2 mM) for 24 h before stimulation with PIC 0.25 $\mu g \cdot mL^{-1}$. After 24h of stimulation, we assessed the development of the antiviral response by measuring ISGs expression by RT-qPCR. All ISGs tested here (IRF1, ISG15, ISG56, ISG54 and ISG12) showed an increase in expression in response to PIC. Also, interestingly, their expression increases in dose response with L-glutamine until it reaches a maximum, which is consistent with the level of expression found in cells cultured in complete DMEM. The difference in expression with cells cultured without L-glutamine was significant as early as 0.2 mM L-glutamine, with levels varying between 2 and 5-fold more, depending on the gene studied **(Figure 2A)**. To validate the effect observed at the transcriptional level, we assessed the synthesis of proteins that rely on the ISRE promoter. Specifically, since we used $A549^{Dual}$, which expresses Lucia luciferase under the control of an ISG54 minimal promoter along with five IFN-stimulated response elements (ISRE), we were able to evaluate ISGs protein expression via luciferase secretion supernatant. Consequently, we examined the release of luciferase into the supernatant of cells treated with PIC by measuring the emitted luminescence using the Lucia luciferase substrate (QUANTI-Luc). Consistent with the results obtained from RT-qPCR, we detected a significant increase in luciferase activity upon PIC stimulation and along with an increase in L-glutamine concentration (up to 10-fold), representing a significant induction of antiviral proteins whose production is under the control of ISRE **(Figure 2B)**.

Oxidative phosphorylation within the mitochondria has been regularly associated with the production of mitochondrial reactive oxygen species (mROS) that have several physiological functions [38]. Among the functions repeatedly associated with these mROS is the promotion of the antiviral response [23,39]. Using MitoSOX™, we explored the formation of mROS in our model by flow cytometry. Thus, after 6h of stimulation with PIC, mROS induction was greater in cells cultured with 2 mM L-glutamine, illustrating the concomitance of this induction with the establishment of the early steps of the antiviral response (**Figure 2C and S1**). Furthermore, this induction was associated with increased TOM20 labeling in A549Dual cells cultured in L-glutamine and treated with PIC for 6h (**Figure**

2D). The increase in TOM20 signal is another manifestation of a more functional mitochondrial network in the presence of L-glutamine, supporting oxidative phosphorylation (**Figure 1**) and induction of mROS (**Figure 2C**).

Furthermore, to confirm that the increase in antiviral response is related to a specific effect of L-glutamine, cells were stimulated with PIC 0.25 $\mu g \cdot mL^{-1}$ in the presence (or absence) of a solution of non-essential amino acids – NEAA (0.1 mM L-alanine, 0.1 mM L-asparagine, 0.1 mM L-aspartic acid, 0.1 mM L-glutamic acid, 0.1 mM glycine, 0.1 mM L-proline and 0.1 mM L-serine) to which 2 mM L-glutamine was added (or not). As shown in **Figure S2**, luciferase activity, and therefore the antiviral response it reflects, was not increased in the presence of NEAA alone. Of note, the addition of L-glutamine to this cocktail restored the previous results.

Surprisingly, the expression of some ISGs does not follow this trend, quite the contrary. Therefore, by evaluating the expression of viperin and 2'-5'-oligoadenylate synthetase 1 (OAS1) by RT-qPCR under the same conditions, we established that these genes are more highly expressed at low L-glutamine concentration. Indeed, their expression decreases inversely (up to 7-fold) with increasing L-glutamine concentration **(Figure 3)**. This suggests that there is in fact a dichotomy in the expression profile of ISGs depending on the predominant metabolic pathway at the time of PIC stimulation. If OXPHOS is favored, through L-glutamine, there will be a greater expression of ISG12, ISG15, ISG54, ISG56 and IRF1. On the contrary, if glycolysis is promoted, in this case in the absence of L-glutamine, other ISGs will be favored, such as OAS1 and viperin. To test the accuracy of this hypothesis, we needed to inhibit these different metabolic pathways under infectious condition and evaluate the development of the antiviral response for the different mentioned ISGs.

3.3. Antiviral response is bivalent and relying alternatively on glycolysis or OXPHOS

As before [22], we used rotenone at a concentration of 1 $\mu g \cdot mL^{-1}$ to inhibit OXPHOS. Since rotenone is a broad-spectrum insecticide, piscicide and pesticide from vegetal origin, known to inhibit the complex I of mitochondrial electron transport chain, thus blocking OXPHOS and associated production of ATP [40]. While 2-DG, at 5 mM was used to inhibit glycolysis. Indeed, 2-DG is a glucose molecule with a 2-hydroxyl group replaced by hydrogen, leading to a molecule unsuitable for glycolysis which competitively inhibits glucose-6-phosphate production by phosphoglucoisomerase [41]. Of note, at the dose of 5 mM 2-DG exerts no cytotoxic effect, assessed by neutral red uptake assay, on $A549^{Dual}$ as shown in **Figure S2.** Thus, we used these inhibitors in combination with stimulation by 0.25 $\mu g \cdot mL^{-1}$ PIC, to study the impact of glycolysis and OXPHOS inhibition on the expression of the antiviral genes presented above.

First, we assessed this expression at the gene level, using RT-qPCR. As before, expression of IRF1, ISG12, ISG15, ISG54 and ISG56 was significantly increased following stimulation with PIC in the presence of 2 mM L-glutamine, compared with cells cultured without L-glutamine **(Figure 4)**. On the contrary, viperin and OAS1 were expressed more when cells were cultured without L-glutamine. The addition of 2-DG, and the subsequent inhibition of glycolysis, resulted in no significant difference in the expression of IRF1, ISG12, ISG15, ISG54 and ISG56. On the other hand, expression of OAS1 and viperin is significantly altered in cells cultured without L-glutamine when glycolysis is inhibited **(Figure 4)**. Therefore, we can conclude that, at the transcriptional level, the expression of genes such as OAS1 and viperin appears to be dependent on glycolysis, whereas the expression of other genes (e.g., ISG12, ISG15, IRF1) is independent of this metabolic pathway. Interestingly, the expression of these same genes is significantly inhibited in the presence of rotenone when cells are cultured with L-glutamine. Their expression level even reached that of cells

cultured without L-glutamine, notably for ISG54 **(Figure 4)**. Regarding OAS1 and viperin, their expression appeared less sensitive to rotenone in cells cultured without L-glutamine, illustrating that these genes are less dependent on OXPHOS than the others **(Figure 4)**. Thus, we have demonstrated here that, at the transcriptional level, the increased expression of certain antiviral genes, such as ISG54 and ISG15, in L-glutamine-cultured cells is related to the higher OXPHOS rate in these cells.

At the protein level, we again studied the luminescence emitted by secreted luciferase in response to PIC to estimate the production of antiviral proteins under the control of the ISRE promoter. The results obtained are consistent with those obtained at the gene level for IRF1, ISG12, ISG15, ISG54 and ISG56. Namely, a decrease in luciferase activity, reflecting a reduction in the production of viral proteins under ISRE control, in response to rotenone treatment **(Figure 5A)**. Finally, by Western blot, we found a higher signal for ISG56 and ISG15 in response to PIC for cells cultured in L-glutamine compared to cells cultured without **(Figure 5B)**. This signal decreased after rotenone treatment, indicating that the up-regulated production of these antiviral proteins in L-glutamine-grown cells is indeed related to higher OXPHOS. Viperin, also assessed by Western blot, follows an opposite pattern. Indeed, cells cultured without L-glutamine show a higher signal in response to PIC, illustrating greater viperin production in these cells than in cells cultured with L-glutamine. However, this production was reduced after inhibition of glycolysis by 2-DG **(Figure 5B)**. Inhibition of OXPHOS by rotenone also appears to alter viperin production at the protein level, whereas no effect was previously shown at the gene level.

3.4. Viperin is expressed in a type I IFN-independent manner in glycolytic condition

In an attempt to explain the specificity of viperin expression, we hypothesized that the viperin promoter region could possibly contain an element enabling greater viperin expression in response to glycolysis. Therefore, we evaluated the expression by RT-qPCR of cytidine / uridine monophosphate kinase 2 (CMPK2) and the lncRNA-negative regulator of the IFN response (lncRNA-NRIR), both of which are expressed at the same time as viperin (**Figure 6A**)[42]. As shown in **Figure 6B**, expression of CMPK2 or lncRNA-NRIR did not vary between L-glutamine and L-glutamine-free conditions. This result corroborates the fact that OAS1 also responds better in glycolysis, even though it does not depend on the same promoter region as viperin.

We then attempted to determine whether the switch that leads to a dichotomy in the ISGs expression profile between cells cultured in L-glutamine versus non-L-glutamine cells could be related to a difference in the expression of type I IFNs between our two conditions. Thus, by RT-qPCR, we assessed IFN-β expression in response to a 6-hour stimulation with PIC, in the presence or absence of L-glutamine. Interestingly, cells cultured without L-glutamine exert an expression of IFN-β similar to that observed for cells cultured with 2 mM L-glutamine (**Figure 6C**). However, this expression is not converted to the protein level, since the signal found for IFN-β is weaker for cells cultured without L-glutamine, whether by Western Blot (**Figure 6D**) or immunofluorescence (**Figure 6E**). The higher expression of IFN-β in cells cultured with 2 mM L-glutamine results in greater STAT2-mediated signaling in these cells compared to cells cultured without L-glutamine, as evidenced by the stronger signal observed for pSTAT2 for this condition (**Figure 6D**). Therefore, higher expression of ISGs such as ISG54, ISG15, or ISG56 would be associated with more efficient IFN-dependent signaling in the presence of L-glutamine. On the other hand, the increase in viperin and OAS1 expression in glycolysis appears to be independent of IFN signaling. At this point, we still assume that it is possible that the higher expression of these two genes in response to PIC under glycolytic conditions may result from the activation of a

transcription factor specific to these two genes compared to the other genes studied here. We therefore sought possible binding sites for transcription factors found in common between the viperin and OAS1 genes on the one hand, and ISG15, ISG54 and ISG12 on the other. To do this, we analyzed a sequence of more than 1000 bp upstream of the first exon of each of these genes, using PROMO tool, based on TRANSFAC 8.3. We then compared the reported binding sites between these two analysis groups (**Figure 6F**). As shown in the Venn diagram, 58 potential binding sites are found to be in common between viperin and OAS1, but only three of these sites are found to be specific to these genes compared to the other ISGs tested: STAT5A, NF-Y, and E2F-1. Therefore, it is possible that one of these three transcription factors is responsible for the expression of viperin and OAS1 in cells treated without L-glutamine.

4. Discussion

With the succession of viral epidemics, some of which have a global impact, research efforts to understand host response mechanisms have intensified. While much progress has been made in understanding the role of metabolism in the activation and function of immune cells, and therefore in understanding how these cells respond to viral infection, depending on their metabolic setting, very little is known about the innate antiviral response of the infected host cell. An interesting question is whether their metabolism influences the canonical antiviral response, namely the IFN response.

It has been established on several occasions that, during viral infection, viruses manipulate host cell metabolism, diverting them from oxidative phosphorylation to glycolysis [21]. This detour has been shown to be of particular interest in viral progeny, as in the case of HIV and DENV [24,43,44]. However, the influence of such hijacking on the production of antiviral effector molecules induced by the IFN response has not yet been explored. The role of glutaminergic metabolism in the antiviral response also remains unresolved in the literature: does the benefit fall to the virus or to the host cell in the event of infection [28]? We have previously shown that OXPHOS promotes the expression of certain antiviral effectors such as ISG54 and ISG56. Furthermore, given that glutaminergic metabolism is closely linked to oxidative phosphorylation through anaplerotic feeding of TCA, we hypothesized here that glutamine intake in an infectious context would increase the antiviral response and the production of antiviral effectors. To address this hypothesis, we stimulated our cells with poly:IC in the presence or absence of L-glutamine, in order to study the intrinsic effect of metabolism on the antiviral response, while avoiding the inhibitory effect that viral proteins can induce during infection.

Here, we were able to demonstrate that cells cultured with 2 mM L-glutamine had more functional mitochondria (**Figure 2D**), which supported greater induction of OXPHOS and mROS induction (**Figures 1 and 2C**). Furthermore, the increased mitochondrial activity in these cells was correlated with a greater production of certain antiviral effectors (ISG12, ISG15, ISG54, ISG56, IRF1), as shown by inhibition of their expression in the presence of rotenone (**Figures 2, 4 and 5**). However, we were also able to show that the expression of certain ISGs escapes the need for OXPHOS, since viperin and OAS1 are more highly expressed in the presence of aerobic glycolysis (**Figures 3, 4 and 5**). One factor that may explain this dichotomy is that IFN-β expression and subsequent signaling are greater in cells to which L-glutamine has been added (**Figure 6**). While higher expression of viperin and OAS1 could be related to a specific transcription factor such as E2F-1 (**Figure 6F**).

It had previously been shown that viperin expression was increased under conditions of high glucose and therefore glycolysis, enabling control of Zika virus infection [45]. These results were surprising in light of our work illustrating the

beneficial effect of OXPHOS on the production of other antiviral effectors such as ISG54 and ISG56 [22]. Our study reconciles these results, as we have demonstrated the existence of a bivalent antiviral response, the orientation of which depends on cellular metabolic status (**Figure 7**). Therefore, OXPHOS in L-glutamine culture favors the production of ISGs such as ISG12, 15, 54 and 56. Whereas, glycolysis is beneficial for the production of viperin and OAS1. These results suggest that the bivalence of the antiviral response may be of interest in the event of metabolic reprogramming by the virus, with one taking over from the other. Thus, in the case of a Warburg-like effect, the host cell can still base its antiviral response on the induction of potent antiviral effectors such as viperin or OAS1. However, through this work we have not been able to uncover the mechanism leading to greater expression of viperin in a glycolytic context. And this important aspect remains to be explored in future work. We hypothesize that the expression of viperin and OAS1 could be linked to the activation of a specific transcription factor in this context. Among those we have identified (**Figure 6F**), it is known that E2F-1 is normally sequestered by retinoblastoma protein (Rb). In the presence of glucose, E2F-1/pRB axis is more active, leading to release of E2F-1 and transcription of its targets [46]. Of note, we have been able to demonstrate that OXPHOS promotes IFN-β production, in contrast to glycolysis, leading to a more efficient production of antiviral effectors. Although viperin gene expression is not affected by OXPHOS inhibition (**Figure 4**), its protein expression appears to be affected (**Figure 5**). Future studies should attempt to shed light on this finding, which may simply be linked to a rotenone effect. Finally, we also found that inhibition of OXPHOS by rotenone did not necessarily result in complete abolition of the expression of OXPHOS-dependent ISGs (**Figures 4 and 5**). This may be due to the fact that the use of rotenone does not result in suppression of mROS induction, since rotenone is sometimes used to induce their induction to a lesser extent [47].

In the light of our initial results, it might be possible to argue that the glutamine addiction discussed in the literature initially seems to go to the host cell, since it produces more antiviral effectors in the presence of L-glutamine. However, since some antiviral effectors can overcome this dependence, it seems that glutamine is more essential to the virus for its progeny [28]. This suggests an adaptive mechanism whereby, to counteract the virus-induced metabolic reprogramming that undermines the antiviral response carried out by ISGs (12, 15, 54 and 56), the host cell has found a way to promote the production of other effectors such as viperin and OAS1. We could be in a frenetic adaptive race in which the cellular metabolic status is of prime importance. These results are encouraging and suggest that the study of glutaminergic metabolism could be an interesting way of approaching the control of a viral infection, and thus exploring possible therapeutic or preventive opportunities. However, these data still need to be consolidated in the case of a real viral infection, especially using viruses of current medical importance, in order to decipher the contribution of L-glutamine and OXPHOS in this case.

Author Contributions

Investigation, resources, data curation, G.L., M.H., A.P.R., D.E.S, P.K.-T. and W.V.; writing—original draft preparation, G.L.; writing—review and editing, G.L., M.H., D.E.S, A.P.R., O.M., P.K.-T., M.R. and W.V.; Methodology, G.L. and W.V.; formal analysis, G.L. and W.V.; supervision, W.V.; Conceptualization, G.L., O.M., and W.V.; funding acquisition, G.L., M.R. and W.V.; All authors have read and agreed to the published version of the manuscript.

Acknowledgments

We would like to thank all our colleagues from PIMIT and DéTROI and especially the Dr. Pascal Baret for his thankful help during this work. Graphical abstract was created using Biorender.com.

Funding

This research was funded by the CASI project (supported by BioST federation of Université de La Réunion). G.L., D.E.S and A.P.R. have PhD degree scholarship from Réunion University (Ecole doctorale STS) funded by DIRED/2021-0161, DIRED/2021-1115 and DIRED/2021-1124 from Région Réunion, respectively. We want to acknowledge the Dr. Philippe Desprès for his thoughtful advices.

Informed Consent Statement

Not applicable.

Data Availability Statement

The data presented in this study are available on request.

Conflicts of Interest

The authors declare no conflict of interest.

References

[1] Ksiazek TG, Erdman D, Goldsmith CS, Zaki SR, Peret T, Emery S, et al. A Novel Coronavirus Associated with Severe Acute Respiratory Syndrome. N Engl J Med 2003;348:1953–66. https://doi.org/10.1056/NEJMoa030781.
[2] Novel Swine-Origin Influenza A (H1N1) Virus Investigation Team, Dawood FS, Jain S, Finelli L, Shaw MW, Lindstrom S, et al. Emergence of a novel swine-origin influenza A (H1N1) virus in humans. N Engl J Med 2009;360:2605–15. https://doi.org/10.1056/NEJMoa0903810.
[3] Zaki AM, van Boheemen S, Bestebroer TM, Osterhaus ADME, Fouchier RAM. Isolation of a Novel Coronavirus from a Man with Pneumonia in Saudi Arabia. N Engl J Med 2012;367:1814–20. https://doi.org/10.1056/NEJMoa1211721.
[4] Baize S, Pannetier D, Oestereich L, Rieger T, Koivogui L, Magassouba N, et al. Emergence of Zaire Ebola Virus Disease in Guinea. New England Journal of Medicine 2014;371:1418–25. https://doi.org/10.1056/NEJMoa1404505.
[5] Faria NR, Azevedo R do S da S, Kraemer MUG, Souza R, Cunha MS, Hill SC, et al. Zika virus in the Americas: Early epidemiological and genetic findings. Science 2016;352:345–9. https://doi.org/10.1126/science.aaf5036.
[6] Zhou P, Yang X-L, Wang X-G, Hu B, Zhang L, Zhang W, et al. A pneumonia outbreak associated with a new coronavirus of probable bat origin. Nature 2020;579:270–3. https://doi.org/10.1038/s41586-020-2012-7.
[7] Thornhill JP, Barkati S, Walmsley S, Rockstroh J, Antinori A, Harrison LB, et al. Monkeypox Virus Infection in Humans across 16 Countries — April–June 2022. New England Journal of Medicine 2022;0:null. https://doi.org/10.1056/NEJMoa2207323.
[8] Majzoub K, Wrensch F, Baumert TF. The Innate Antiviral Response in Animals: An Evolutionary Perspective from Flagellates to Humans. Viruses 2019;11:758. https://doi.org/10.3390/v11080758.
[9] Chow KT, Gale M, Loo Y-M. RIG-I and Other RNA Sensors in Antiviral Immunity. Annu Rev Immunol 2018;36:667–94. https://doi.org/10.1146/annurev-immunol-042617-053309.
[10] Motwani M, Pesiridis S, Fitzgerald KA. DNA sensing by the cGAS–STING pathway in health and disease. Nat Rev Genet 2019;20:657–74. https://doi.org/10.1038/s41576-019-0151-1.
[11] Schoggins JW. Interferon-Stimulated Genes: What Do They All Do? Annu Rev Virol 2019;6:567–84. https://doi.org/10.1146/annurev-virology-092818-015756.
[12] Schneider WM, Chevillotte MD, Rice CM. Interferon-Stimulated Genes: A Complex Web of Host Defenses. Annu Rev Immunol 2014;32:513–45. https://doi.org/10.1146/annurev-immunol-032713-120231.
[13] Dixit E, Boulant S, Zhang Y, Lee ASY, Odendall C, Shum B, et al. Peroxisomes Are Signaling Platforms for Antiviral Innate Immunity. Cell 2010;141:668–81. https://doi.org/10.1016/j.cell.2010.04.018.
[14] Odendall C, Dixit E, Stavru F, Bierne H, Franz KM, Durbin AF, et al. Diverse intracellular pathogens activate type III interferon expression from peroxisomes. Nat Immunol 2014;15:717–26. https://doi.org/10.1038/ni.2915.
[15] Schoggins JW, Rice CM. Interferon-stimulated genes and their antiviral effector functions. Current Opinion in Virology 2011;1:519–25. https://doi.org/10.1016/j.coviro.2011.10.008.
[16] McNab F, Mayer-Barber K, Sher A, Wack A, O'Garra A. Type I interferons in infectious disease. Nat Rev Immunol 2015;15:87–103. https://doi.org/10.1038/nri3787.
[17] Beyer DK, Forero A. Mechanisms of Antiviral Immune Evasion of SARS-CoV-2. Journal of Molecular Biology 2022;434:167265. https://doi.org/10.1016/j.jmb.2021.167265.
[18] Meylan E, Curran J, Hofmann K, Moradpour D, Binder M, Bartenschlager R, et al. Cardif is an adaptor protein in the RIG-I antiviral pathway and is targeted by hepatitis C virus. Nature 2005;437:1167–72. https://doi.org/10.1038/nature04193.
[19] Mesev EV, LeDesma RA, Ploss A. Decoding type I and III interferon signalling during viral infection. Nat Microbiol 2019;4:914–24. https://doi.org/10.1038/s41564-019-0421-x.
[20] Loftus RM, Finlay DK. Immunometabolism: Cellular Metabolism Turns Immune Regulator. Journal of Biological Chemistry 2016;291:1–10. https://doi.org/10.1074/jbc.R115.693903.
[21] Thaker SK, Ch'ng J, Christofk HR. Viral hijacking of cellular metabolism. BMC Biology 2019;17:59. https://doi.org/10.1186/s12915-019-0678-9.

[22] Lebeau G, El Safadi D, Paulo-Ramos A, Hoareau M, Desprès P, Krejbich-Trotot P, et al. The Efficient Antiviral Response of A549 Cells Is Enhanced When Mitochondrial Respiration Is Promoted. Pathogens 2022;11:1168. https://doi.org/10.3390/pathogens11101168.
[23] Buskiewicz IA, Montgomery T, Yasewicz EC, Huber SA, Murphy MP, Hartley RC, et al. Reactive oxygen species induce virus-independent MAVS oligomerization in systemic lupus erythematosus. Sci Signal 2016;9. https://doi.org/10.1126/scisignal.aaf1933.
[24] Angin M, Volant S, Passaes C, Lecuroux C, Monceaux V, Dillies M-A, et al. Metabolic plasticity of HIV-specific CD8 + T cells is associated with enhanced antiviral potential and natural control of HIV-1 infection. Nature Metabolism 2019;1:704–16. https://doi.org/10.1038/s42255-019-0081-4.
[25] Chatel-Chaix L, Cortese M, Romero-Brey I, Bender S, Neufeldt CJ, Fischl W, et al. Dengue Virus Perturbs Mitochondrial Morphodynamics to Dampen Innate Immune Responses. Cell Host & Microbe 2016;20:342–56. https://doi.org/10.1016/j.chom.2016.07.008.
[26] Carneiro L, Guissard C, Offer G, Belenguer P, Pénicaud L, Leloup C. The mitochondrial fission induced by glucose is essential to the ROS signaling in hypothalamic detection of hyperglycemia. Diabetes & Metabolism 2010;36:A38. https://doi.org/10.1016/S1262-3636(10)70145-2.
[27] Zhang W, Wang G, Xu Z-G, Tu H, Hu F, Dai J, et al. Lactate Is a Natural Suppressor of RLR Signaling by Targeting MAVS. Cell 2019;178:176-189.e15. https://doi.org/10.1016/j.cell.2019.05.003.
[28] Koufaris C, Nicolaidou V. Glutamine addiction in virus-infected mammalian cells: A target of the innate immune system? Med Hypotheses 2021;153:110620. https://doi.org/10.1016/j.mehy.2021.110620.
[29] Shiratori R, Furuichi K, Yamaguchi M, Miyazaki N, Aoki H, Chibana H, et al. Glycolytic suppression dramatically changes the intracellular metabolic profile of multiple cancer cell lines in a mitochondrial metabolism-dependent manner. Sci Rep 2019;9:18699. https://doi.org/10.1038/s41598-019-55296-3.
[30] Repetto G, del Peso A, Zurita JL. Neutral red uptake assay for the estimation of cell viability/cytotoxicity. Nat Protoc 2008;3:1125–31. https://doi.org/10.1038/nprot.2008.75.
[31] Yang Y, Zhang G, Yang T, Gan J, Xu L, Yang H. A flow-cytometry-based protocol for detection of mitochondrial ROS production under hypoxia. STAR Protocols 2021;2:100466. https://doi.org/10.1016/j.xpro.2021.100466.
[32] Messeguer X, Escudero R, Farré D, Núñez O, Martínez J, Albà MM. PROMO: detection of known transcription regulatory elements using species-tailored searches. Bioinformatics 2002;18:333–4. https://doi.org/10.1093/bioinformatics/18.2.333.
[33] Farré D, Roset R, Huerta M, Adsuara JE, Roselló L, Albà MM, et al. Identification of patterns in biological sequences at the ALGGEN server: PROMO and MALGEN. Nucleic Acids Research 2003;31:3651–3. https://doi.org/10.1093/nar/gkg605.
[34] Martin FJ, Amode MR, Aneja A, Austine-Orimoloye O, Azov AG, Barnes I, et al. Ensembl 2023. Nucleic Acids Research 2023;51:D933–41. https://doi.org/10.1093/nar/gkac958.
[35] Heberle H, Meirelles GV, Da Silva FR, Telles GP, Minghim R. InteractiVenn: a web-based tool for the analysis of sets through Venn diagrams. BMC Bioinformatics 2015;16:169. https://doi.org/10.1186/s12859-015-0611-3.
[36] Gitlin L, Barchet W, Gilfillan S, Cella M, Beutler B, Flavell RA, et al. Essential role of mda-5 in type I IFN responses to polyriboinosinic:polyribocytidylic acid and encephalomyocarditis picornavirus. Proc Natl Acad Sci U S A 2006;103:8459–64. https://doi.org/10.1073/pnas.0603082103.
[37] Kato H, Sato S, Yoneyama M, Yamamoto M, Uematsu S, Matsui K, et al. Cell type-specific involvement of RIG-I in antiviral response. Immunity 2005;23:19–28. https://doi.org/10.1016/j.immuni.2005.04.010.
[38] Zorov DB, Juhaszova M, Sollott SJ. Mitochondrial Reactive Oxygen Species (ROS) and ROS-Induced ROS Release. Physiological Reviews 2014;94:909–50. https://doi.org/10.1152/physrev.00026.2013.
[39] Nobre L, Wise D, Ron D, Volmer R. Modulation of Innate Immune Signalling by Lipid-Mediated MAVS Transmembrane Domain Oligomerization. PLoS ONE 2015;10:e0136883. https://doi.org/10.1371/journal.pone.0136883.
[40] Heinz S, Freyberger A, Lawrenz B, Schladt L, Schmuck G, Ellinger-Ziegelbauer H. Mechanistic Investigations of the Mitochondrial Complex I Inhibitor Rotenone in the Context of Pharmacological and Safety Evaluation. Sci Rep 2017;7:45465. https://doi.org/10.1038/srep45465.
[41] Wick AN, Drury DR, Nakada HI, Wolfe JB. Localization of the primary metabolic block produced by 2-deoxyglucose. J Biol Chem 1957;224:963–9.
[42] Kambara H, Niazi F, Kostadinova L, Moonka DK, Siegel CT, Post AB, et al. Negative regulation of the interferon response by an interferon-induced long non-coding RNA. Nucleic Acids Research 2014;42:10668–80. https://doi.org/10.1093/nar/gku713.
[43] Fontaine KA, Sanchez EL, Camarda R, Lagunoff M. Dengue Virus Induces and Requires Glycolysis for Optimal Replication. Journal of Virology 2015;89:2358–66. https://doi.org/10.1128/JVI.02309-14.
[44] Valle-Casuso JC, Angin M, Volant S, Passaes C, Monceaux V, Mikhailova A, et al. Cellular Metabolism Is a Major Determinant of HIV-1 Reservoir Seeding in CD4+ T Cells and Offers an Opportunity to Tackle Infection. Cell Metabolism 2019;29:611-626.e5. https://doi.org/10.1016/j.cmet.2018.11.015.
[45] Reslan A, Haddad JG, Desprès P, Bascands J-L, Gadea G. High Glucose Induces in HK2 Kidney Cells an IFN–Dependent ZIKV Antiviral Status Fueled by Viperin. Biomedicines 2022;10:1577. https://doi.org/10.3390/biomedicines10071577.
[46] Almacellas E, Pelletier J, Manzano A, Gentilella A, Ambrosio S, Mauvezin C, et al. Phosphofructokinases Axis Controls Glucose-Dependent mTORC1 Activation Driven by E2F1. IScience 2019;20:434–48. https://doi.org/10.1016/j.isci.2019.09.040.
[47] Li N, Ragheb K, Lawler G, Sturgis J, Rajwa B, Melendez JA, et al. Mitochondrial Complex I Inhibitor Rotenone Induces Apoptosis through Enhancing Mitochondrial Reactive Oxygen Species Production. Journal of Biological Chemistry 2003;278:8516–25. https://doi.org/10.1074/jbc.M210432200.

Figures

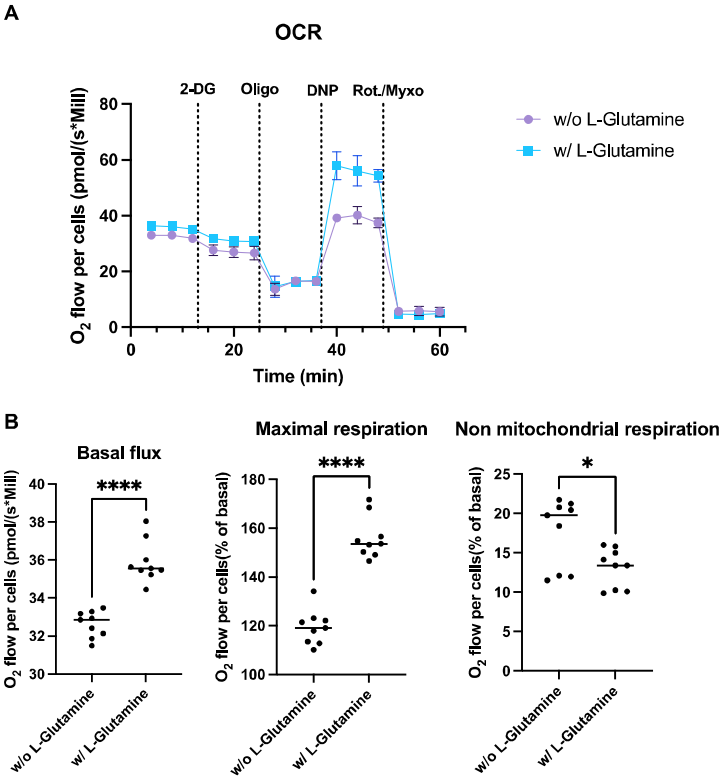

Figure 1 – OXPHOS is associated with L-glutamine-containing medium. (A) Comparison of the oxygen consumption rate of A549^{Dual} cultured with or without L-glutamine. 5 mM 2-deoxyglucose (2-DG) has been used to inhibit hexokinase activity and glycolysis. 1 µM oligomycin (Oligo) has been used to inhibit ATP synthase. 100 µM 2,4-dinitrophenol (DNP) has been used as protonophoric uncoupler, allowing maximal respiration. 1 µM Rotenone – 1 µM Myxothiazol has been used to uncouple both mitochondrial complex I and III, illustrating non mitochondrial respiration. The metabolism of cells grown in RPMI supplemented with 2 mM L-glutamine is more dependent on oxidative phosphorylation. (B) More specifically, cells cultured with L-glutamine have higher basal O_2 consumption flux, associated with higher maximal respiration capacity and consistently lower non mitochondrial respiration. Error bars represent standard errors of three independent experiments. *$p<0.0332$; **** $p<0.0001$.

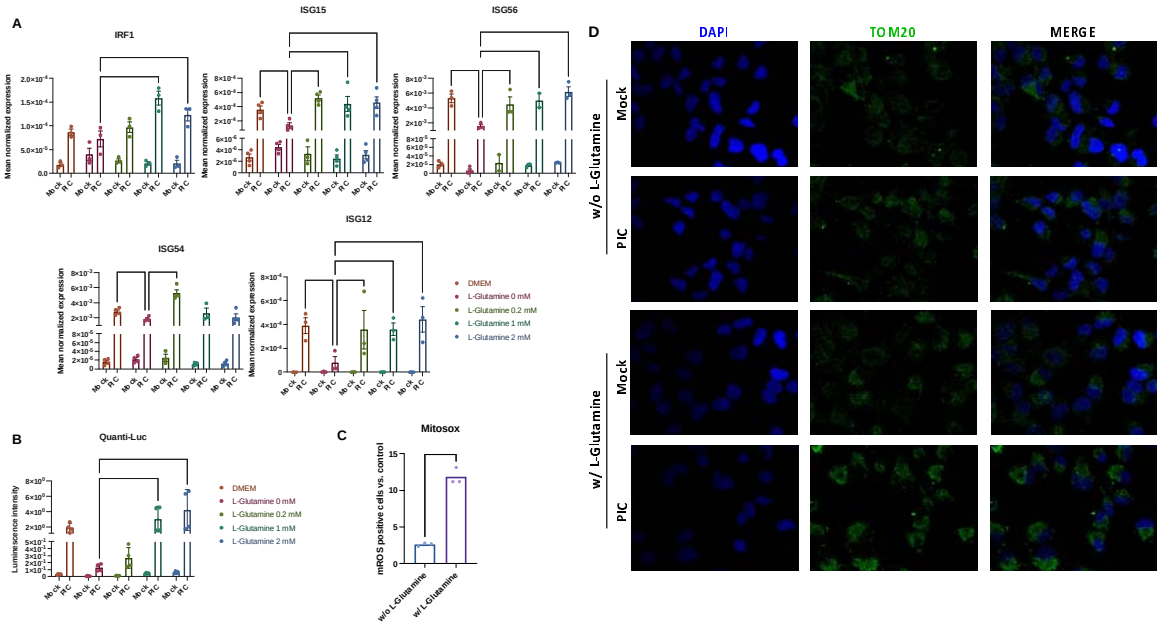

Figure 2 – L-glutamine increases antiviral response to poly:IC. (A) L-glutamine related overexpression of ISGs expression. The expression of several ISGs (IRF1, ISG15, ISG56, ISG54, ISG12) has been assessed by RT-qPCR after 24-hour stimulation of A549^{Dual}, grown in RPMI 2 g·L^{-1} glucose, supplemented with increasing doses of L-glutamine (0, 0.2, 1 and 2 mM), using PIC 0.25 µg·mL^{-1}. Results are expressed as mean normalized expression, following normalization with expression of 18S ribosomal RNA as a housekeeping gene. (B) ISRE-dependent proteins increased production in presence of L-glutamine. Evaluation of IRF pathway activation in response to PIC 0.25 µg·mL^{-1} stimulation of A549^{Dual} grown in RPMI 2 g·L^{-1} glucose supplemented with increasing doses of L-glutamine (0, 0.2, 1 and 2 mM) was achieved by measuring activity of secreted Lucia luciferase, using QUANTI-Luc substrate 24 hours after treatment. Results are expressed as emitted luminescence intensity. (C) mROS induction is higher in presence of L-glutamine. Mitochondrial ROS were measured with MitoSOX™ Red using a flow cytometry-based protocol in cells grown in RPMI 2 g·L^{-1} glucose, supplemented or not with 2 mM L-glutamine, after 6h of stimulation with PIC. Error bars represent standard errors of three independent experiments. *p<0.0332; ** p<0.0021; *** p<0.0002; **** p<0.0001. (D) Increased OXPHOS is associated with higher mitochondrial TOM20 labeling. TOM20 expression was assessed by immunofluorescence in A549^{Dual}, grown in RPMI 2 g·L^{-1} glucose, supplemented or not with 2 mM, using PIC 0.25 µg·mL^{-1}. These images are representative of three independent experiments.

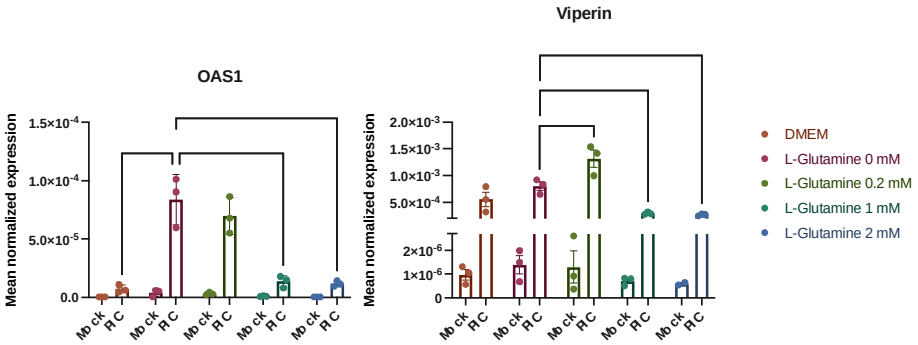

Figure 3 – Expression of OAS1 and viperin are independent L-glutamine. Expression of OAS1 and viperin was assessed by RT-qPCR following a 24-hour stimulation of A549^{Dual}, grown in RPMI 2 g·L^{-1} glucose, supplemented with increasing doses of L-glutamine (0, 0.2, 1 and 2 mM), using PIC 0.25 µg·mL^{-1}. Results are expressed as mean normalized expression, following normalization with expression of 18S ribosomal RNA as a housekeeping gene. Error bars represent standard errors of three independent experiments. *** $p<0.0002$; **** $p<0.0001$.

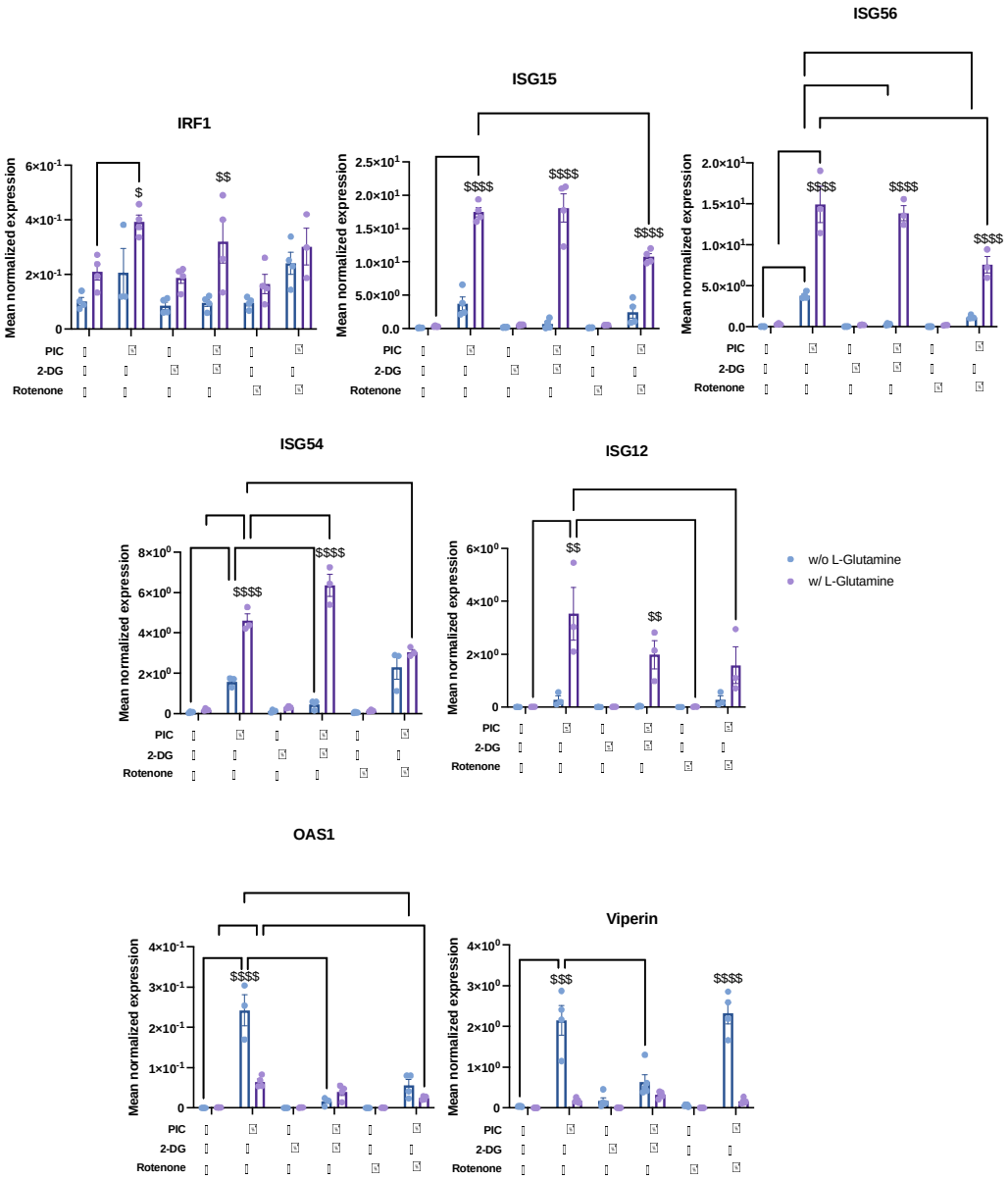

Figure 4 – Bivalent expression of ISGs is based on glycolysis and OXPHOS. Expression of several ISGs (IRF1, ISG15, ISG56, ISG54, ISG12, OAS1 and viperin) have been assessed by RT-qPCR following a 24-hour stimulation of A549^{Dual}, grown in RPMI 2 g·L^{-1} glucose, supplemented or not with 2 mM L-glutamine, using PIC 0.25 µg·mL^{-1}. Simultaneously, to evaluate the influence of glycolysis and OXPHOS on the upregulation of ISGs regarding L-glutamine supplementation, 5 mM 2-deoxyglucose (2-DG) and 1 µg·mL^{-1} were used to inhibit glycolysis and OXPHOS respectively. Results are expressed as mean normalized expression, following normalization with expression of RNA polymerase II RNA as a housekeeping gene. The error bars represent standard errors of three independent experiments. *p<0.0332; ** p<0.0021; *** p<0.0002; **** p<0.0001 as compared to PIC. $^{\$}$ p<0.0332; $^{\$\$}$ p<0.0021; $^{\$\$\$}$ p<0.0002; $^{\$\$\$\$}$ p<0.0001 comparison between without L-glutamine vs. with L-glutamine.

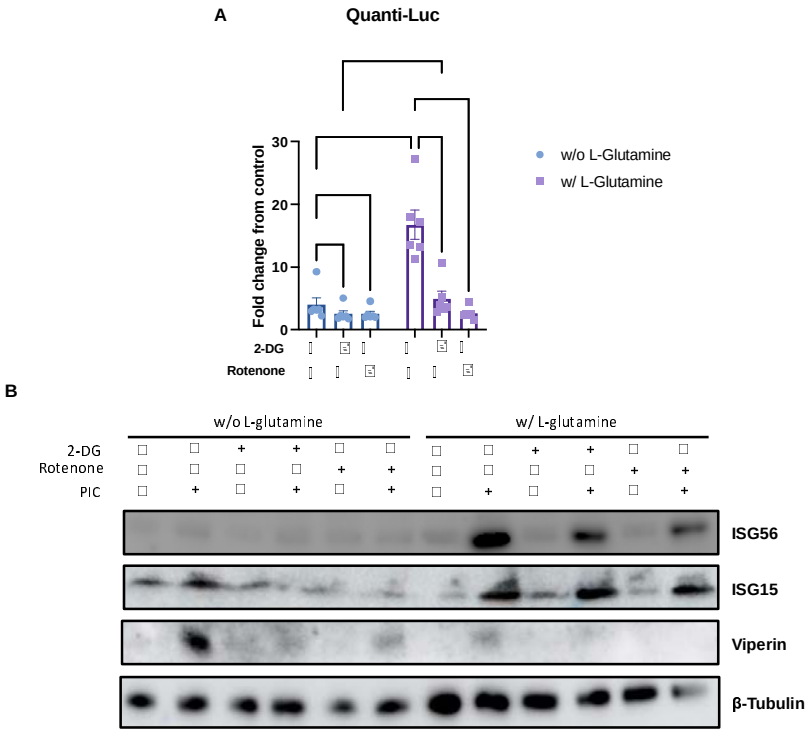

Figure 5 – Bivalent ISG production depends on glycolysis or OXPHOS. (A) ISRE-dependent proteins increased production in presence of L-glutamine is linked to OXPHOS. Evaluation of IRF pathway activation in response to PIC 0.25 µg·mL^{-1} stimulation of A549^{Dual} grown in RPMI 2 g·L^{-1} glucose, supplemented or not with 2 mM L-glutamine, was achieved by measuring activity of secreted Lucia luciferase, using QUANTI-Luc substrate 24 hours after treatment. Concomitantly, to assess the influence of glycolysis and OXPHOS on the upregulation of ISGs with respect to L-glutamine supplementation, 5 mM 2-deoxyglucose (2-DG) and 1 µg·mL^{-1} were used to inhibit glycolysis and OXPHOS. Results are expressed as emitted luminescence intensity. Error bars represent standard errors from three independent experiments. ** $p<0.0021$; *** $p<0.0002$. (B) Bivalent production of ISGs relies on either glycolysis or OXPHOS. ISGs production in response to PIC 0.25 µg·mL^{-1} stimulation of A549^{Dual} grown in RPMI 2 g·L^{-1} glucose, supplemented or not with 2 mM L-glutamine, was achieved by western blot analysis. Western blot assay was achieved with mouse anti-ISG56, rabbit anti-ISG15, mouse anti-viperin and rabbit anti-β-tubulin antibodies. These images are representative of three independent experiments.

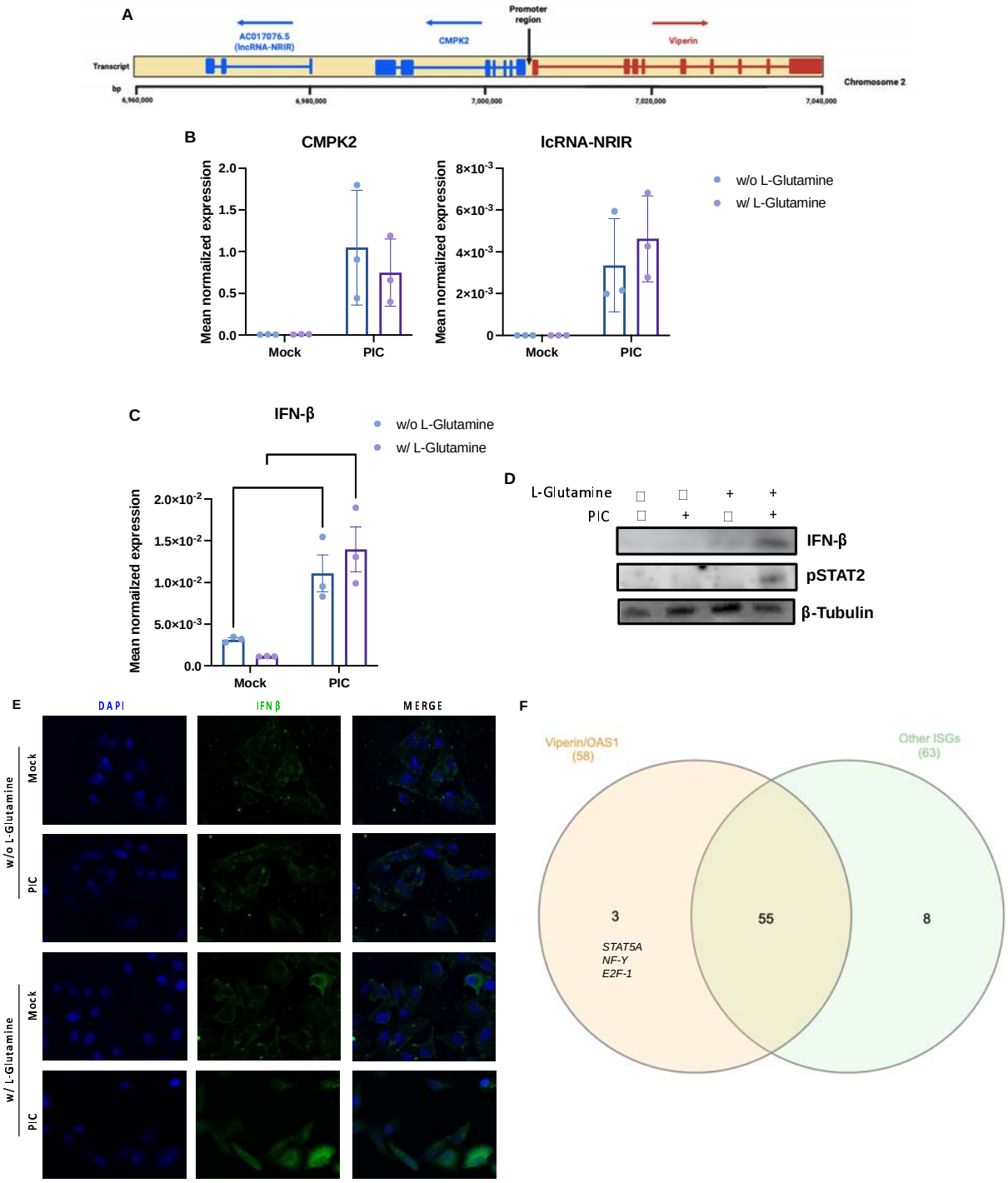

Figure 6 – Differential expression of ISGs correlates with variable IFN-β signaling. (A) Schematic representation of viperin, CMPK2 and lc-NRIR loci on chromosome 2. Exon/intron structure of genes is represented, promoter region is annotated and arrows indicate the orientation of transcription for each locus. (B) CMPK2 and lc-NRIR are expressed in the same manner under glycolytic and OXPHOS conditions. The expression of CMPK2 and lc-NRIR has been assessed by RT-qPCR after 24-hour stimulation of A549^{Dual}, grown in RPMI 2 g·L^{-1} glucose, supplemented or not 2 mM L-glutamine, using PIC 0.25 µg·mL^{-1}. Results are expressed as mean normalized expression, following normalization with expression of RNA polymerase II RNA as a housekeeping gene. (C) IFN-β mRNA has the same level of expression under glycolytic and OXPHOS conditions. The expression of IFN-β has been assessed by RT-qPCR after 6-hour stimulation of A549^{Dual}, grown in RPMI 2 g·L^{-1} glucose, supplemented or not with 2 mM L-glutamine, using PIC 0.25 µg·mL^{-1}. Results are expressed as mean normalized expression, following normalization

with expression of RNA polymerase II RNA as a housekeeping gene. Error bars represent standard errors from three independent experiments. * $p<0.0332$; ** $p<0.0021$. (D, E) Alternative ISGs expression is related to IFN-β production and signaling. IFN-β production and phosphorylation of STAT2 in response to PIC stimulation of $A549^{Dual}$ grown in RPMI 2 $g \cdot L^{-1}$ glucose, supplemented or not with 2 mM L-glutamine, was achieved by western blot analysis and immunofluorescence. Western blot assay was achieved with mouse anti-IFN-β, rabbit anti-pSTAT2, and rabbit anti-β-tubulin antibodies. Immunofluorescence assay was achieved using mouse anti-IFN-β, donkey anti-mouse Alexa 488 and DAPI. These images are representative of three independent experiments. (F) Overexpression of viperin and OAS1 could be related to specific transcription factors activation under glycolytic condition. On one hand, we compared the promoter region, of viperin and OAS1 and on the other hand the promoter region of ISG12, ISG15 and ISG54, using PROMO tool based on TRANSFAC 8.3, looking for potential transcription factor binding sites. As represented, we determine three potential transcription factors that are specific for viperin and OAS1: STAT5A, NF-Y and E2F-1.

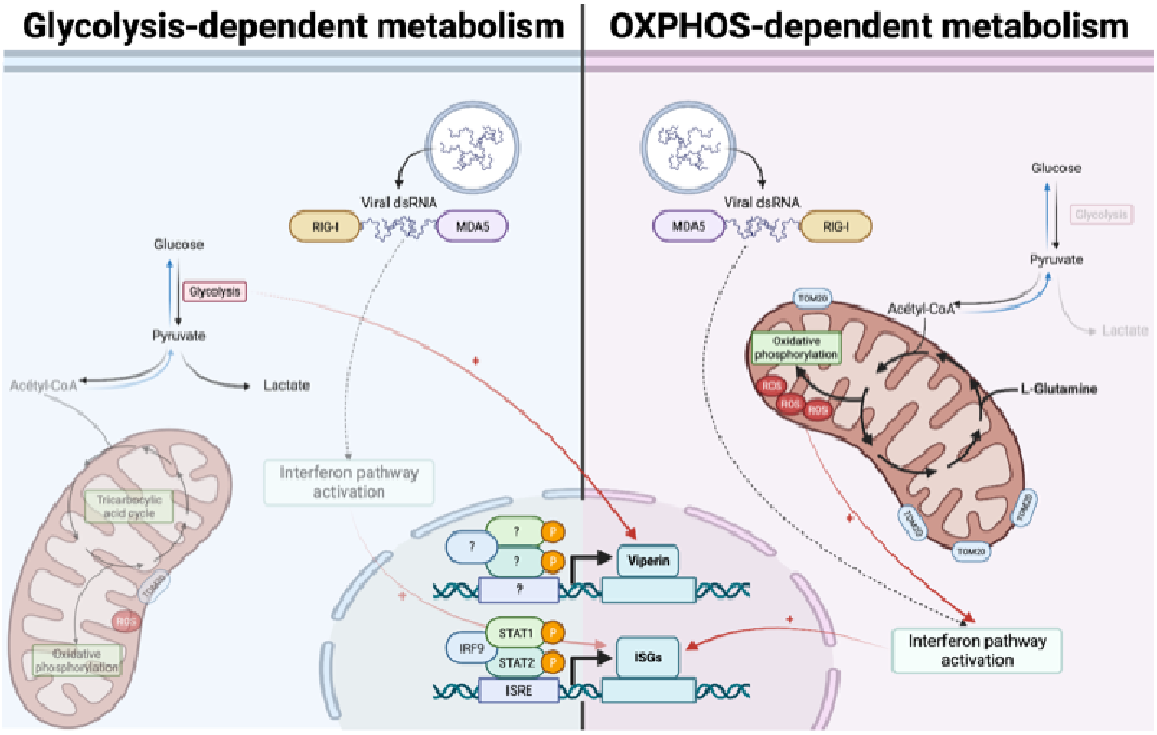

Figure 7 – Bidirectional ISGs expression is based on differential metabolic states. In cells relying on OXPHOS, antiviral response mounting is related to more functional mitochondria, leading to higher expression of ISGs. On the contrary, in cells relying on glycolysis, less efficient interferon signaling is associated with less functional mitochondria and consequently lower ISGs expression. Viperin and OAS1 escape this process and are more expressed in glycolysis-dependent cells, independently from interferon β.

Supplementary material

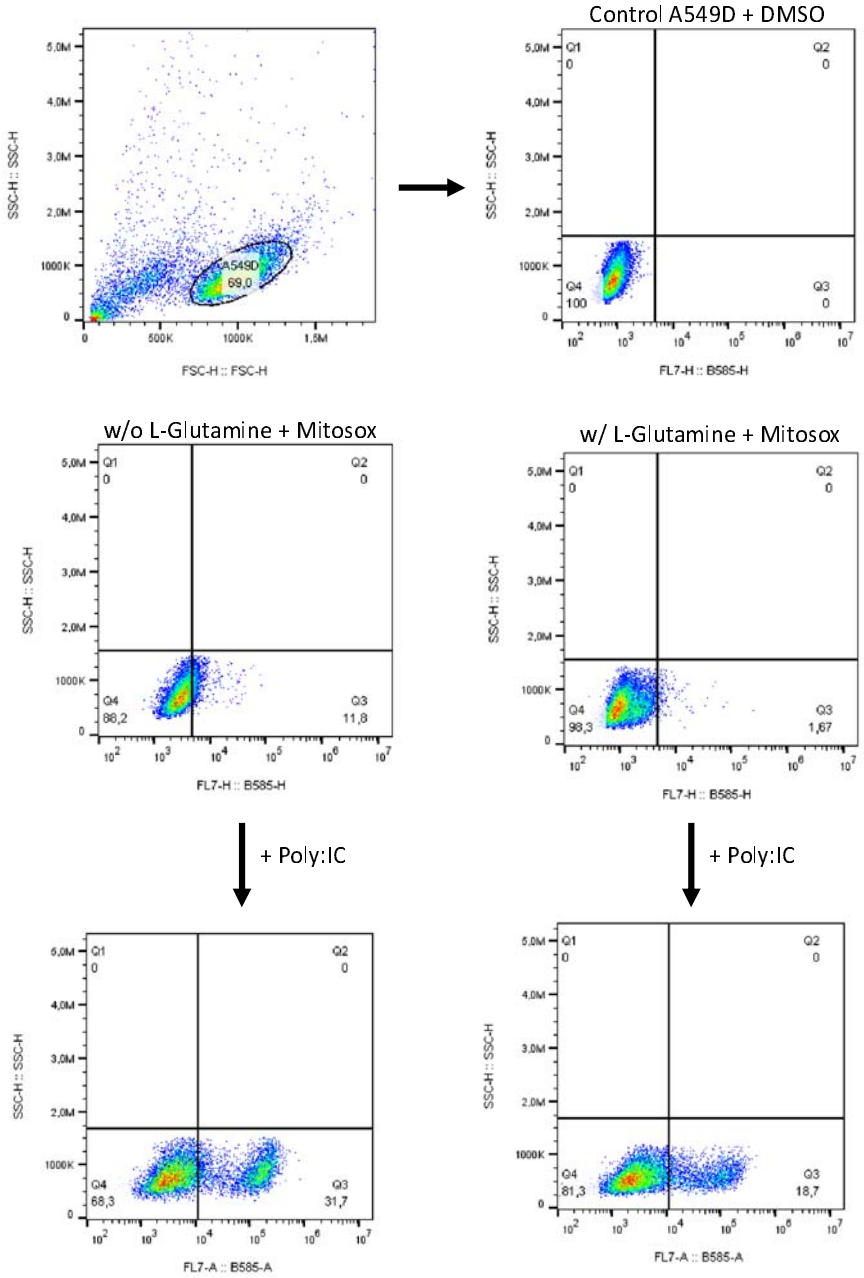

Figure S1 – Gating strategy for flow cytometry-based MitoSOX™ Red assay. Living A549^{Dual} were stained with MitoSOX™ Red at a final concentration of 5 µM, after a stimulation of 6 hour with PIC 0.25 µg·mL^{-1}. Cells were gated by using forward scatter versus side scatter and mitochondrial ROS induction was assessed based on positive signal in PE channel.

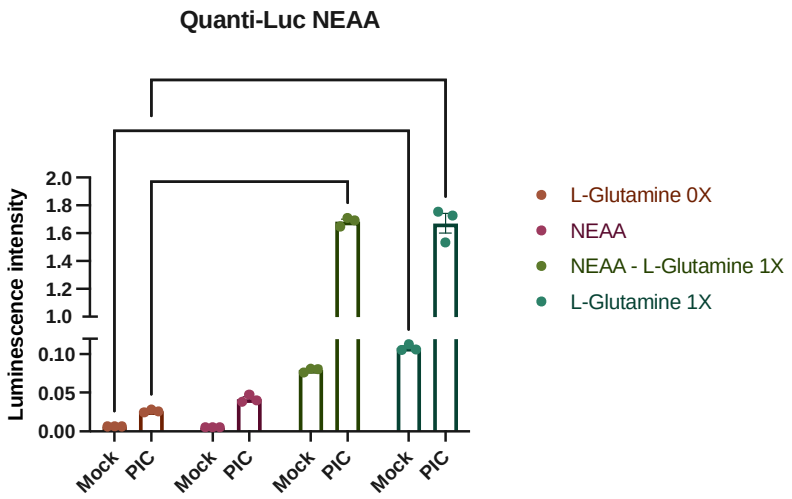

Figure S2 – Antiviral response upregulation is independent of non-essential amino acids. Evaluation of IRF pathway activation in response to PIC 0.25 µg·mL^{-1} stimulation of A549^{Dual} grown in RPMI 2 g·L^{-1} glucose supplemented with either or both non-essential amino acids – NEAA and 2 mM L-glutamine, was achieved by measuring activity of secreted Lucia luciferase, using QUANTI-Luc substrate 24 hours after treatment. Results are expressed as emitted luminescence intensity. Error bars represent standard errors of three independent experiments. *p<0.0332; ** p<0.0021; *** p<0.0002; **** p<0.0001.

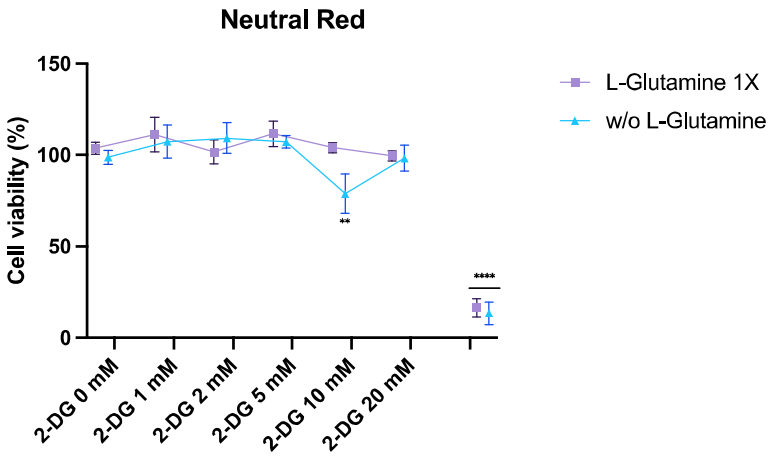

Figure S3 – 2-deoxyglucose exerts no cytotoxic effect. We treated A549^{Dual} with 2-deoxyglucose with concentrations ranging from 1 mM to 20 mM for 24 hours. We then evaluated the impact of these different concentrations on cell viability by neutral red assay.

.